Roles of Conformational and Configurational Defects on the Physical Aging of Amorphous Poly(lactic acid)

Kaoru Aou[†] and Shaw Ling Hsu*

Department of Polymer Science and Engineering and Materials Research Science and Engineering Center, University of Massachusetts, Amherst, Massachusetts 01003

Lothar W. Kleiner and Fuh-Wei Tang

Abbott Vascular, Cardiac Therapies, 3200 Lakeside Drive, Santa Clara, California 95054

Received: June 11, 2007; In Final Form: August 8, 2007

The roles of poly(lactic acid) chain conformation and configuration on the enthalpy relaxation kinetics of amorphous poly(lactic acid) were examined. Enthalpic relaxation data, which were scaled to the same supercooling from the initial fictive temperature, were taken for three types of the polymer containing various D-lactyl monomers (5.7%, 13.0%, 50%) to assess the effects of configurational defects. The kinetics data were very similar from sample to sample. The effects of configurational defects were assessed using the generalized Kohlrausch−Williams−Watts (KWW) equation solved by the Tool−Narayanaswamy−Moynihan (TNM) equation. The major effect of increasing the D-lactyl contents was to lower the PLA glass transition temperature, thereby accelerating the kinetics of enthalpic relaxation. Configurational defects showed no significant effect on the other KWW/TNM fit parameters (x, Δh, ln A). A slightly larger KWW β stretched exponential parameter is observed for greater (50% D) than for lower (5.7% D) amount of D-lactyl monomer, although these differences are just within the experimental error. Raman spectroscopy showed that conformation does not change appreciably during physical aging.

Introduction

The changes in mechanical and transport properties, which accompany physical aging,[1,2] are critically relevant to both industrial and medical applications of poly(lactic acid), or PLA. This polymer, derived from renewable resources,[3,4] was recently introduced in commercial applications as a viable commodity-scale thermoplastic.[5−7] PLA has also been studied as a drug-carrier matrix in drug delivery systems as well as the bulk component of other medical devices as it has been established to be biocompatible and bioresorbable.[8−11] It is important to understand the kinetics of PLA physical aging and its impact on the performance of PLA-based drug delivery systems, as it impacts device shelf life, which needs to be evaluated for any pharmaceutical device.

Physical aging is the densification, or isotropic volumetric shrinkage, of amorphous materials below their glass transition temperature. This is in contrast to anisotropic shrinkage, in particular fiber shrinkage, which we previously studied using a spectroscopic method and in relation to molecular deformation in PLA fibers.[12] The same method, originally developed in another study,[7] is used here to evaluate any changes in the rotational isomeric populations of PLA during physical aging, in order to determine any changes in PLA conformation during physical aging. Conformational changes have been reported to cease below the glass transition for polystyrene and poly(methyl methacrylate),[13,14] as reported from wide-angle X-ray scattering, whereas others have used a model that assumes conformational changes during physical aging.[15,16] There are also studies based on thermal density fluctuations, which show that physical aging is accompanied by an increase in local order.[17,18] Therefore, it was important to study whether or not conformational changes are observable during the physical aging of PLA.

We are also interested in the effect of configurational defects, or polymer tacticity, on the kinetics of physical aging. To our knowledge, there are only a few studies, namely, on poly(methyl methacrylate), that report an effect of polymer tacticity on the activation enthalpy.[19,20] The effect of stereochemical defects on physical aging is a relatively unexplored and important aspect that we pursue through this study. From our past investigations, we know that D-lactyl defects perturb the distribution of rotational isomer populations at D−L junctions, thereby rendering the overall chain more flexible.[21] We know that a greater fraction of configurational defects leads to lower glass transition temperatures (T_g), which speeds up the kinetics of physical aging. We wish to see any effects of these defects above and beyond this change in the T_g.

PLA amorphous dynamics have previously been studied using dielectric spectroscopy and calorimetric methods.[22−27] However, no well-known physical aging models were used to analyze those aging kinetics data. We use the generalized Kohlrausch−Williams−Watts (KWW) equation, solved by the Tool−Narayanaswamy−Moynihan (TNM) description of relaxation time, to characterize the physical aging kinetics of PLA, as it is an accepted model for analysis of physical aging.[28−30] In this study, calorimetric methods are employed to monitor enthalpic relaxation of PLA, which is a measure of physical aging.

Materials and Experimental Techniques

Materials. Poly(DL-lactic acid), or PLA50, was obtained from Abbott Vascular, Inc. Poly(L-lactic acid) with 5.7% D, or

* To whom correspondence should be addressed. Phone: 413-577-1125. E-mail: slhsu@polysci.umass.edu.

[†] Current address: PU Global Product R&D, The Dow Chemical Company, Freeport, TX 77541.

10.1021/jp074509t CCC: $37.00
Published on Web 10/04/2007

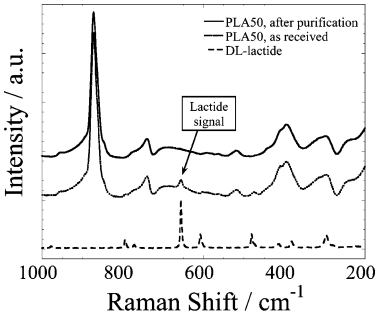

Figure 1. Raman spectra of DL-lactide, PLA50 pellet as-received, and PLA50 after purification.

PLA5.7, and 13.0% D-lactyl content, or PLA13, were received from NatureWorks and were the same samples used in previous studies.[21] The D-lactyl contents were chosen such that quiescent crystallization was slow and crystallization could be readily suppressed by a rapid thermal quench, at the same time covering a wide range of tacticity. Residual lactides were found for the as-received PLA50 sample, as indicated in its Raman spectra by the extra peak at 656 cm^{-1}, as shown in Figure 1. DL-Lactide was used as received from Aldrich. The PLA50 sample was therefore purified by first preparing a solution in dichloromethane at a concentration of 10% by weight and then precipitating in methanol. The sample was dried in ambient atmosphere and then further dried in vacuum at 60 °C for 2 h. Raman spectra of the resulting samples were taken to ensure that no solvent peaks are present. The same treatment was performed for the PLA13 and PLA5.7 samples.

Molecular Weight Characterization. An in-house-assembled size exclusion chromatograph was used to measure the molecular weight parameters of various PLA samples. A Knauer HPLC pump K-501 and a Polymer Laboratories PL DataStream detector were used on a Polymer Laboratories 5 μm mixed-D column, with chloroform at 30 °C as the eluting medium. Narrow molecular weight polystyrene standards ranging from 2.7 to 390 kg mol^{-1} were used for calibration.

Differential Scanning Calorimetry. A TA Instruments model Q100 differential scanning calorimeter equipped with an RCS cooling system and nitrogen gas purge set at 50 mL/min flow rate was used for all calorimetric measurements. Aluminum pans with PLA samples were hermetically sealed before measurement. Polymer sample masses varied from 6 to 13 mg. The top part of the pan was pressed down to improve thermal contact with the sample, taking care that the flatness of the bottom face contacting the temperature sensor in the differential scanning calorimetry (DSC) chamber was maintained. Indium and water were used as a standard to calibrate the temperature at their onset melting points of 156.6 and 0.0 °C, respectively. The indium heat of fusion (28.6 J g^{-1}) was used to calibrate heat flow.[31] Heat flow and not absolute heat capacity was the quantity measured, since for the purposes of enthalpy relaxation kinetics, it was only necessary to measure the total heat release.[19] The difference between heat flows of aged samples and quenched glass was integrated over a temperature interval of 10−100 °C to compute the excess enthalpy that characterizes the extent of physical aging, in accordance with the method used by Petrie.[32] The "glass transition temperature" in heating scans was taken as the halfway point of the tangent line containing the inflection point and hereafter referred to as $T_{g,h}$. The fictive temperature option available on the Universal Analysis software from TA Instruments was not used, in large part because in our measurements, the value thus measured did not differ by more than 0.05 °C compared with $T_{g,h}$. The onset of glass transition upon cooling, or $T_{g,onset}$, has been taken to be the temperature of the intersection point between the liquid baseline and the glass transition inflection point in constant rate cooling scans.

Dispersive Raman Microspectroscopy. A Jobin-Yvon Horiba LabRam HR800 dispersive Raman spectrometer was used to obtain Raman spectra of PLA50. The 632.8 nm line of the helium−neon gas laser was used for excitation. A spectral resolution of 4 cm^{-1} was maintained near the laser line. Circularly polarized incident light was obtained with a quarter-wave retardation plate in order to perform a signal averaging over all possible orientations. For the purposes of acquiring temperature-dependent Raman spectra, an in-house-built aluminum heating block was used. A copper−constantan thermocouple (diameter ∼0.08 mm), calibrated with boiling water (100.0 °C) and ice water (0.0 °C), was placed close to the sample for temperature measurement. The PLA50 sample was further wrapped with aluminum foil for good thermal conduction, with a small hole at the top (∼2 mm) to allow for Raman spectral acquisition. The sample was conditioned at 55 °C (well above both its glass transition and fictive temperatures) for 1.5 h to initialize thermal history to the equilibrium liquid state.

Computer Program for Curve Fitting to KWW/TNM Equations. A computer program code written in Visual Basics for Applications (VBA) was implemented in a spreadsheet written in Microsoft Excel 2000. This VBA program was used to fit the data to the nonlinear, generalized KWW/TNM equations. A standard Levenberg−Marquardt algorithm was used to fit the experimental aging data to those equations.[33,34]

Modeling

In order to evaluate the effect of configurational defects, the theories on physical aging kinetics are reviewed. The aging behavior of small molecular glass and atactic polymers has been studied extensively in the past. Many phenomenological models of sub-glass-transition amorphous dynamics exist.[28−30,35,36] One that is commonly encountered in literature is the Cowie−Ferguson equation,[37] or the linear KWW equation, which requires a simple linear three-parameter fit and has been used most often with small molecular and inorganic glasses.[38,39] Its theoretical explanation has been presented with minimal assumptions,[40] which is the major reason for its adoption in the interpretation of physical aging in many systems. However, the linear KWW equation has problems in theory and in application in the context of enthalpic relaxation.[41] In fact, the asymmetry-of-approach and the memory effect experiments by Kovacs showed that experimental phenomena could not be explained by a constant relaxation time,[36,42] which means that a variable relaxation time has to be incorporated in any aging kinetics model. A recent study also indicates that the fit value of ΔH_{endo} approaching time infinity from a linear KWW analysis of short-time data cannot predict the equilibrium value of ΔH_{endo} that was obtained experimentally.[43]

In order to reconcile nonlinear effects, the generalized KWW equation and TNM formalism for relaxation time are used to analyze the physical aging most commonly of polymeric glasses.[28−30,36] The TNM model modifies the Arrhenius equation by incorporating the fictive temperature as a measure of the instantaneous structure, in addition to the annealing temperature, of the material during aging. The generalized KWW equation is expressed as follows:

$$\delta(T_a, t)/\delta(T_a, 0) = \exp[-(\int_0^t dt/\tau_0(T, t))^{\beta}] \quad (1)$$

where δ/δ_0 represents the deviation from thermodynamic equilibrium, t is the aging time, τ_0 is the characteristic relaxation time (variable over the course of enthalpic relaxation), and β is a stretched exponential parameter. The calorimetric δ/δ_0 is calculated from experimental quantities as follows:

$$\delta(T_a, t)/\delta(T_a, 0) = (\Delta H_\infty - \Delta H_t)/\Delta H_\infty \quad (2)$$

where ΔH_∞ is the endotherm at long time (equilibrium) and ΔH_t is the endotherm at time t. As eq 1 is not solvable analytically for known expressions of the relaxation time, it is numerically solved. The solution uses the well-known TNM equation,[28,29,36] which has temperature- (T_a) and structure-dependent (T_f) terms:

$$\ln \tau_0 = \ln A + \frac{x\Delta h}{RT_a} + \frac{(1-x)\Delta h}{RT_f(\delta)} \quad (3)$$

where ln A is a pre-exponential factor, R is the universal gas constant, T_a is the annealing temperature, Δh is the activation energy for enthalpy relaxation, and x partitions the temperature and structure terms. T_f is the instantaneous fictive temperature of the material that represents the instantaneous structure of the glass during aging, as shown:

$$T_f(\delta) = T_f(T_a, t) = T_a + \frac{\delta(T_a, t)}{\Delta C_p} \quad (4)$$

where T_a is the aging temperature and ΔC_p is the change in heat capacity as the system passes through the glass transition temperature. Although there are criticisms concerning the shortcoming of the model,[37,44,45] this is the preferred model used in studies of polymer physical aging.[46,47]

In the actual application of the TNM formalism to the analysis of physical aging, finding a stable solution can be problematic if a four-parameter fit (β, x, Δh, ln A) is adopted. This owes to the fact that the solution can be overly sensitive to experimental error. This aspect is remedied by reducing the data analysis to a three-parameter fit. This is done by fixing one of the parameters out of the four-parameter fit. It has been noted previously that, due to the fact that T_a/T_f is close to unity on the absolute temperature scale, then eq 3 simplifies to

$$\ln \tau_0 \approx \ln A + \frac{\Delta h}{RT} \quad (5)$$

where $T_a \sim T_f \sim T$ so that two of the fitting parameters (ln A and Δh) would be correlated linearly.[19] Owing to this correlation, the curve fit becomes extremely sensitive to small changes in δ (of the order of magnitude of experimental uncertainty). To address this issue, the following approximation was used:[48]

$$\frac{d \ln|q|}{d(1/T_{g,onset})} \approx -\frac{\Delta h}{R} \quad (6)$$

where q is the cooling rate and $T_{g,onset}$ is the onset of glass transition. The parameter Δh was thus determined from a set of cooling rate dependence experiments, the result of which is summarized in Figure 2. The activation energy for enthalpy relaxation obtained through eq 6 for amorphous PLA of varying tacticity was in the range of 750−900 kJ/mol for the three PLA samples, which was on the same order of magnitude as, or higher than, for other polymers.[47,49−51] With the value of Δh determined, the analysis of enthalpic relaxation now involves a stable three-parameter fit.

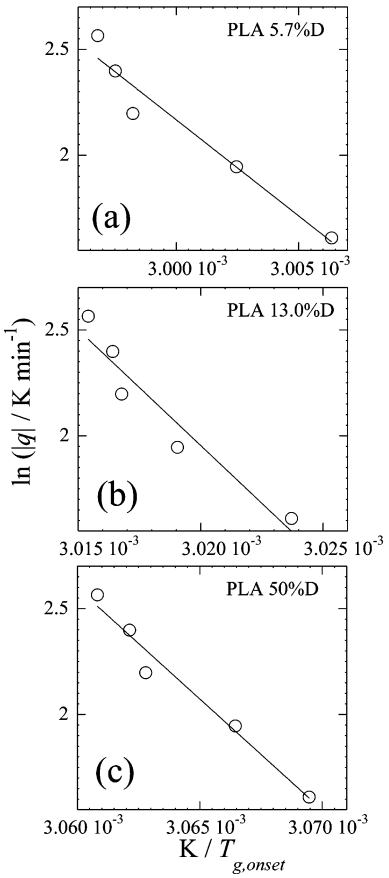

Figure 2. Determination of the TNM Δh parameter by the cooling rate dependence of the onset of the glass transition for (a) PLA 5.7% D, (b) 13.0% D, and (c) 50% D. The uncertainty of Δh is stated as one standard deviation.

Results and Discussion

The PLA samples were measured using size exclusion chromatography in order to assess their molecular weight and molecular weight distribution. Mark Houwink parameters of (K/mL g^{-1}, a) = (4.9×10^{-3}, 0.794) were used for polystyrene,[52] whereas (5.45×10^{-2}, 0.73) and (2.27×10^{-2}, 0.77) were used for all-L and DL-PLA, respectively.[53] The result is shown in Table 1. It is noted that the molecular weights are all above the entanglement molecular weight of 8700 and 10 500 g mol^{-1} of a PLA melt (reported at 180 and 200 °C, respectively).[54,55] DSC was used to obtain the $T_{g,h}$ of all the samples so that subsequent physical aging studies are done for each samples at nearly the same supercooling from the respective $T_{g,h}$ values. In addition, with different heating rate, the heat capacity change at the glass transition (ΔC_p) did not vary more than 2%,[2,19] and the aging endotherm (ΔH_{endo}) at a given time and temperature also did not vary significantly (see Table 2). The average of the ΔC_p value for the different heating rates was used in the analysis of enthalpy relaxation kinetics. We then further studied the role of conformational and configurational defects of these samples associated with physical aging.

From past studies we know that the conformer distribution is perturbed by D-lactyl configurational defects.[21] Here, in the context of physical aging, we were more concerned with the change in the conformer distribution during physical aging rather than the difference in the initial values of the *tg*'*t* conformer population of the PLA samples of varying tacticity. We used a

TABLE 1: Summary of Molecular Weights and Glass Transition Temperatures of PLA Samples

	PLLA standard			PDLLA standard			
	M_n/kg mol^{-1}	M_w/kg mol^{-1}	PDI	M_n/kg mol^{-1}	M_w/kg mol^{-1}	PDI	$T_{g,h}$/°C at 10 °C min^{-1}
PLA 5.7% D	35	69	1.96	46	87	1.90	59.3
PLA 13.0% D	33	65	1.95	43	82	1.90	58.4
PLA 50% D	n/a	n/a	n/a	21	40	1.92	53.0

TABLE 2: Summary of ΔC_p and ΔH_{endo} of the Three PLA Samples at 5, 10, and 20 °C Min^{-1} Heating Rates

	PLA 5.7% D (T_a = 46.0 °C)			PLA 13.0% D (T_a = 45.0 °C)			PLA 50% D (T_a = 40.0 °C)		
heating rate/°C min^{-1}	5	10	20	5	10	20	5	10	20
ΔH_{endo} after 30 min aging at T_a	1.1	1.2	1.2	1.1	1.2	1.2	1.0	1.2	1.2
ΔC_p at $T_{g,h}$/J g^{-1} °C^{-1}	0.54	0.54	0.54	0.53	0.52	0.52	0.53	0.54	0.53
$T_{g,h}$/°C	58.3	59.3	61.3	57.2	58.4	60.7	51.8	53.0	54.9

method from our previous studies, which relied on the fact that ratio of the Raman spectral intensities at the 1128 and 1044 cm^{-1} can be related linearly with the *tg*′*t* conformer population.[7,56] The conformer population of the PLA50 was observed as a function of time at 37 °C during the physical aging process. In the annealing time range and beyond where the DSC results from Figure 3 show that physical aging is underway, Raman spectra from Figure 4 shows no discernible difference during physical aging at 37 °C. This is especially true in the present case where there are no detectable differences in the *tg*′*t* population during physical aging. This is consistent with what has been observed for other amorphous polymers, where neither interchain spacing nor conformation change below their glass transition temperatures.[13,14] However, we should recognize the possibility that the changes in conformer population are small and therefore experimentally undetectable. This may result from the fact that the *tg*′*t* conformer (∼80%) is dominant in PLA.[7,56]

Therefore, conformational defects have little or no detectable role in physical aging of PLA. On the other hand, configurational defects are known to lower the T_g of PLA by as much as 10 °C and therefore are expected to have significant impact on the aging kinetics. In addition, any impact of configurational defects beyond their effect on the T_g was studied. To analyze these effects of configurational defects, DSC was used, as relatively small samples needed to be tested.[46] When referring specifically to physical aging measured through DSC, the term enthalpic relaxation would be used. The experimental details and analysis of excess enthalpy using calorimetry is not as trivial as in the case of crystallinity analysis, and the issues are discussed here.

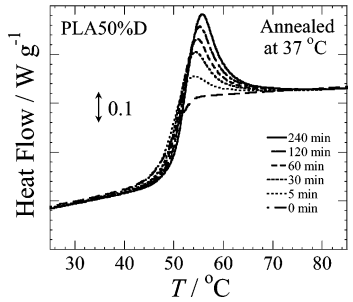

Figure 3. DSC traces of PLA 50% D annealed at 37.0 °C. Conditioning took place after initializing thermal history at 120 °C for 1 min. Heating rate is 20 °C min^{-1}.

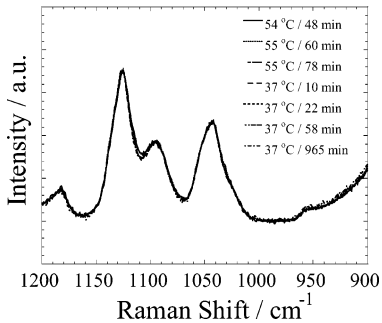

Figure 4. Raman spectra of PLA50 during physical aging at 37.0 °C. The sample was preconditioned at 55 °C for 1.5 h to remove thermal history.

Enthalpic relaxation kinetics is very sensitive to its thermal history, and therefore certain precautions needed to be taken. After every heating scan, the sample was quenched to 0 °C at the maximum cooling rate accessible by the equipment (∼40 °C/min near T_g), before reheating to the annealing temperature for physical aging. This was done to approach the annealing temperature from the low-temperature side, which would minimize the extent of aging prior to reaching isothermal conditions,[46] as well as to suppress crystallization for the PLA5.7 sample, which can crystallize when cooled down slowly from the melt. Also, in order to initialize the thermal history of the sample at the melt state, heating scans were performed in the temperature range of 0 to 120, 160, and 160 °C for PLA50, PLA13, and PLA5.7, respectively.

The difference between annealing temperature and the glass transition is a very important parameter to consider, since enthalpic relaxation kinetics accelerates as the temperature approaches the glass transition. The purpose of measuring $T_{g,h}$ was to determine the set of supercooling temperatures to use for the annealing temperatures with respect to the approximate $T_{g,h}$ of the sample. Later measurement of $T_{g,h}$ upon cooling at 5 °C min^{-1} yielded values that were separated by about the same amount from sample to sample. In order to evaluate the enthalpy relaxation kinetics, the initial fictive temperature is necessary, and this is determined by the equilibrium excess enthalpy for samples annealed at 5 °C lower than the $T_{g,h}$.[46,47] It should be noted that true glass transition temperature in practice is determined during cooling scans;[57] however, as our purpose does not lie in the determination of the true glass transition temperature, this was not done.

As annealing required isothermal conditions, stability of temperature as well as reproducibility of data were examined. Sub-T_g annealing was performed in the DSC cell for the same sample at temperatures 14, 12, 10, 7, and 5 °C lower than the $T_{g,h}$, and aging experiments conducted under identical conditions (annealing time and temperature) were repeated three times. Data were reproducible as shown in Figure 5. The cell temperature was stable to ±0.02 °C for isothermal tests programmed at 30.0, 40.0, and 50.0 °C for 10 min, and the temperature range covers the set of annealing temperatures used in the present study. Heating scans of melt-quenched states were compared before and after the set of aging experiments were carried out to

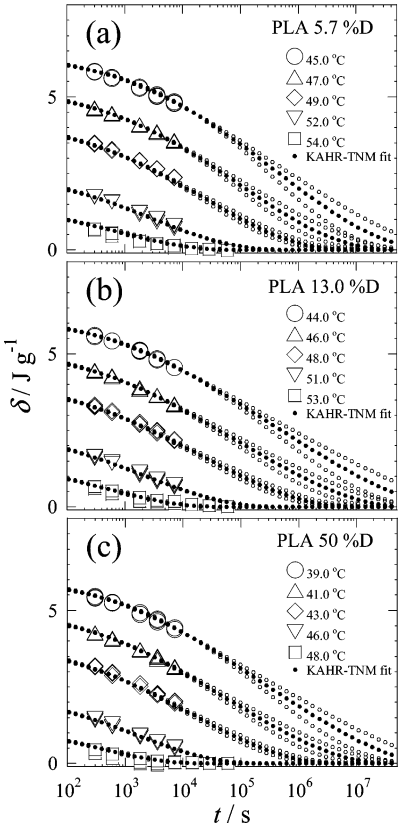

Figure 5. Extent of enthalpy relaxation as a function of time for (a) PLA 5.7% D, (b) PLA 13.0% D, and (c) PLA 50% D. The black dotted lines represent the curve fit to the generalized KWW/TNM equations. The gray dotted lines correspond to the upper and lower uncertainty limits of the Δh of each sample.

TABLE 3: TNM Fitting Parameters for PLA 5.7% D, 13.0% D, and 50% D

	PLA 5.7% D	PLA 13.0% D	PLA 50% D
$T_{f,o}$/°C	56.9	55.9	50.4
$\Delta h/10^4$ J mol^{-1}	76 ± 15	91 ± 16	87 ± 15
x	0.63 ∓ 0.15	0.47 ∓ 0.11	0.48 ∓ 0.11
β	0.41 ± 0.05	0.49 ± 0.07	0.51 ± 0.08
ln(A/s)	−272 ∓ 55	−328 ∓ 59	−319 ∓ 56

confirm the absence of sample degradation due to the DSC heating scans.

In the context of physical aging/enthalpic relaxation, the most significant effect of configurational defects on the PLA backbone may be their effect on the T_g,[58] which in turn affects the enthalpic relaxation kinetics. Comparing the samples of PLA5.7 and PLA50, we find that the addition of more D-lactyl units resulted in the lowering of $T_{g,h}$ by about 6 °C, as seen from Table 2. Consequently, the initial fictive temperature ($T_{f,o}$) is also lowered by about 6 °C, as shown in Table 3. Since physical aging occurs only below T_g, where glassy behavior is observed, then for a given annealing temperature, enthalpic relaxation of PLA50 should proceed faster than that of PLA5.7, all other things being equal. So a difference in T_g in fact should have a very large impact on aging kinetics.

In order to investigate effects of configurational defects above and beyond their impact on T_g, the experiments were set up such that a series of approximately constant supercoolings relative to $T_{g,h}$, which is related to the $T_{f,o}$, were applied to the three types of PLA samples to facilitate comparison of enthalpic relaxation kinetics. The KWW/TNM equations require $T_{f,o}$ to be included as a parameter so that using these equations allow us to separate the two effects of configurational defects on the enthalpic relaxation kinetics: one on the T_g, and thus $T_{f,o}$, and the other on the KWW/TNM fit parameters.

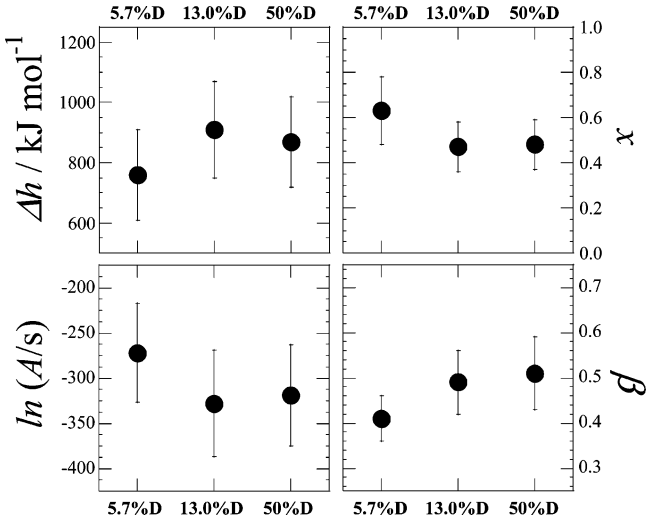

Figure 6. KWW/TNM fitting parameters of PLA 5.7% D, 13.0% D, and 50% D. The error bars correspond to the upper and lower uncertainty limits of the Δh of each sample.

The data and curve of best fit to the KWW/TNM equations are presented in Figure 5. We note that it is difficult to discern an obvious difference in enthalpy relaxation kinetics between the three different samples. The KWW/TNM fitting parameters are shown in Figure 6. The error bars of Δh in that figure correspond to the propagation of the curve-fitting error combined with the experimental error, as shown in Figure 2. The error bars for the other three parameters in Figure 6 represent the lower and higher values obtained when the Δh parameter is used in the KWW/TNM fit is fixed to its lower or higher value. For clarity, the actual values are tabulated in Table 3. We note that smaller error bars may be achieved if both the curve-fitting and experimental errors were reduced, which can be accomplished if a greater range of cooling rates were covered in obtaining the value of Δh. In future attempts, one must still keep in mind that too slow a cooling rate would be affected by noise of the calorimeter, while too fast a cooling rate could suffer from thermal lags that would render the measured values of $T_{g,onset}$ meaningless. That is, there is a limited range of cooling rates under which meaningful values of Δh can be determined.

Figure 6 shows that aside from β, none of the fitting parameters are different beyond the uncertainty limits. Since the values of Δh and ln A are correlated to each other, then their uncertainties would also be correlated. Unless the Δh were determined to higher accuracies, the sample-to-sample differences for these two parameters would not be distinguishable. The x parameter, which partitions the relaxation time into temperature- and structure-dependent terms, also does not vary beyond significance across the different PLA samples. Since the physical meaning of x is not well understood, further analysis is difficult at this point.

From Figure 6, we find that the β parameter is all within experimental error for the three PLA samples. The relative magnitude for PLA13 compared with the other two samples is not obvious owing to its large uncertainty. It should be kept in mind that a β value of about 0.5 has been found in polystyrene where KWW/TNM analysis was used, with the Δh determined separately as in the present study.[43] However, as the value of β is just within the error bar for PLA5.7 and PLA50, it merits some discussion, since it is conceivable that difference may be significant if the uncertainty of Δh can be reduced in future

experiments. There is the possibility that the difference is simply due to the fact that PLA5.7 can crystallize, whereas PLA50 cannot.[59] However, as care was taken to suppress crystallization by quenching rapidly from the melt, and subsequent DSC scans showed no detectable crystallinity, there is the possibility that difference in crystallinity does not exist and cannot explain the difference in β. In order to explain the difference in the β parameter, it has been suggested that in glassy polymers there is a crossover size limit ("Gaussian blobs") between Rouse dynamics ($\beta = 0.5$) and α-relaxation dynamics ($\beta < 0.5$).[60−63] In those studies, it is proposed that Rouse dynamics is dominant above, and α-relaxation dynamics below, the crossover limit.[64,65] If the precision obtained for the values of β are improved through better estimation of Δh and there are significant differences between the β values, then this crossover size limit concept should certainly be revisited in greater depth.

Conclusions

Conformational analysis using Raman spectroscopy reveals little or no change in helical *tg't* conformer population during the physical aging process, which is consistent with previous observations of other polymers. We find that the use of cooling rate dependence of $T_{g,onset}$ to obtain the activation energy for enthalpy relaxation (Δh) is required in order to have a stable and reliable curve fit. The values of Δh were therefore calculated for each PLA sample and had similar magnitude as other polymeric glasses. The effects of polymer tacticity on the KWW/TNM fit parameters were analyzed. The major effect of configurational defects was to lower the $T_{g,h}$ of PLA, thereby accelerating the enthalpic relaxation kinetics at a given annealing temperature. All KWW/TNM fit parameters were found not to change significantly from sample to sample. Further attempts to improve accuracy of the Δh and thus of the curve-fitting parameters should be done in the future.

Acknowledgment. We thank the National Science Foundation Materials Research Science and Engineering Center at the University of Massachusetts as well as Bioabsorbable Vascular Solutions, a subsidiary of Abbott Laboratories, for financial support. We also thank Jed Randall of NatureWorks for providing the PLA samples of different tacticity.

References and Notes

(1) Struik, L. C. E. *Physical Aging in Amorphous Polymers and Other Materials*; Elsevier Scientific Publishing Company: New York, 1978.
(2) McKenna, G. B. Glass Formation and Glassy Behavior. In *Polymer Properties*; Booth, C., Price, C., Eds.; Pergamon Press: New York, 1989; Vol. 2, p 311.
(3) Vink, E. T. H.; Rabago, K. R.; Glassner, D. A.; Gruber, P. R. *Polym. Degrad. Stab.* **2003**, *80*, 403.
(4) Mecking, S. *Angew. Chem., Int. Ed.* **2004**, *43*, 1078.
(5) Smith, P. B.; Leugers, A.; Kang, S.; Hsu, S. L.; Yang, X. *J. Appl. Polym. Sci.* **2001**, *82*, 2497.
(6) Smith, P. B.; Leugers, A.; Kang, S.; Yang, X.; Hsu, S. L. *Macromol. Symp.* **2001**, *175*, 81.
(7) Yang, X.; Kang, S.; Yang, Y.; Aou, K.; Hsu, S. L. *Polymer* **2004**, *45*, 4241.
(8) Wood, D. A. *Int. J. Pharm.* **1980**, *7*, 1.
(9) Schakenraad, J. M.; Oosterbaan, J. A.; Nieuwenhuis, P.; Molenaar, I.; Olijslager, J.; Potman, W.; Eenink, M. J. D.; Feijen, J. *Biomaterials* **1988**, *9*, 116.
(10) Jain, R.; Shah, N. H.; Malick, A. W.; Rhodes, C. T. *Drug Dev. Ind. Pharm.* **1998**, *24*, 703.
(11) Jain, R. A. *Biomaterials* **2000**, *21*, 2475.
(12) Aou, K.; Kang, S.; Hsu, S. L. *Macromolecules* **2005**, *38*, 7730.
(13) Krimm, S. *J. Phys. Chem.* **1953**, *57*, 22.
(14) Krimm, S.; Tobolsky, A. V. *J. Polym. Sci.* **1951**, *6*, 667.
(15) Robertson, R. E. *J. Polym. Sci., Polym. Phys. Ed.* **1979**, *17*, 597.
(16) Robertson, R. E.; Simha, R.; Curro, J. G. *Macromolecules* **1984**, *17*, 911.
(17) Roe, R. J.; Curro, J. J. *Macromolecules* **1983**, *16*, 428.
(18) Song, H. H.; Roe, R. J. *Macromolecules* **1987**, *20*, 2723.
(19) Hodge, I. M. *J. Non-Cryst. Solids* **1994**, *169*, 211.
(20) Doulut, S.; Bacharan, C.; Demont, P.; Bernes, A.; Lacabanne, C. *J. Non-Cryst. Solids* **1998**, *235*, 645.
(21) Kang, S.; Zhang, G.; Aou, K.; Hsu, S. L.; Stidham, H. D.; Yang, X. *J. Chem. Phys.* **2003**, *118*, 3430.
(22) Celli, A.; Scandola, M. *Polymer* **1992**, *33*, 2699.
(23) Liao, K. R.; Quan, D. P.; Lu, Z. J. *Eur. Polym. J.* **2002**, *38*, 157.
(24) Rosilio, V.; Deyme, M.; Benoit, J. P.; Madelmont, G. *Pharm. Res.* **1998**, *15*, 794.
(25) Teramoto, Y.; Nishio, Y. *Biomacromolecules* **2004**, *5*, 397.
(26) Quan, D. P.; Liao, K. R.; Zhao, J. H. *Acta Polym. Sin.* **2004**, 726.
(27) Cai, H.; Dave, V.; Gross, R. A.; McCarthy, S. P. *J. Polym. Sci., Part B: Polym. Phys.* **1996**, *34*, 2701.
(28) Narayanaswamy, O. S. *J. Am. Ceram. Soc.* **1971**, *54*, 491.
(29) Moynihan, C. T.; Macedo, P. B.; Montrose, C. J.; Gupta, P. K.; DeBolt, M. A.; Dill, J. F.; Dom, B. E.; Drake, P. W.; Esteal, A. J.; Elterman, P. B.; Moeller, R. P.; Sasabe, H.; Wilder, J. A. *Ann. N.Y. Acad. Sci.* **1976**, *279*, 15.
(30) Kovacs, A. J.; Aklonis, J. J.; Hutchinson, J. M.; Ramos, A. R. *J. Polym. Sci., Polym. Phys. Ed.* **1979**, *17*, 1097.
(31) *CRC Handbook of Chemistry and Physics*; Lide, D. R., Ed.; CRC Press: Boca Raton, FL, 1999.
(32) Petrie, S. E. B. *J. Polym. Sci., Part A−2* **1972**, *10*, 1255.
(33) Levenberg, K. *Q. Appl. Math.* **1944**, *2*, 164.
(34) Marquardt, D. W. *J. Soc. Ind. Appl. Math.* **1963**, *11*, 431.
(35) Williams, G.; Watts, D. C. *Trans. Faraday Soc.* **1970**, *66*, 80.
(36) Tool, A. Q. *J. Am. Ceram. Soc.* **1946**, *29*, 240.
(37) Cowie, J. M. G.; Ferguson, R. *Polymer* **1995**, *36*, 4159.
(38) Xia, X. Y.; Wolynes, P. G. *Phys. Rev. Lett.* **2001**, *86*, 5526.
(39) Dixon, P. K.; Nagel, S. R. *Phys. Rev. Lett.* **1988**, *61*, 341.
(40) Palmer, R. G.; Stein, D. L.; Abrahams, E.; Anderson, P. W. *Phys. Rev. Lett.* **1984**, *53*, 958.
(41) Hutchinson, J. M.; Kumar, P. *Thermochim. Acta* **2002**, *391*, 197.
(42) Kovacs, A. J. *Adv. Polym. Sci.* **1964**, *3*, 394.
(43) Li, Q. X.; Simon, S. L. *Polymer* **2006**, *47*, 4781.
(44) O'Reilly, J. M.; Hodge, I. M. *J. Non-Cryst. Solids* **1991**, *131*, 451.
(45) Simon, S. L.; Bernazzani, P. *J. Non-Cryst. Solids* **2006**, *352*, 4763.
(46) Hutchinson, J. M. *Prog. Polym. Sci.* **1995**, *20*, 703.
(47) Simon, S. L.; Sobieski, J. W.; Plazek, D. J. *Polymer* **2001**, *42*, 2555.
(48) Moynihan, C. T.; Easteal, A. J.; Wilder, J.; Tucker, J. *J. Phys. Chem.* **1974**, *78*, 2673.
(49) Biddlestone, F.; Harris, A.; Hay, J. N.; Hammond, T. *Polym. Int.* **1996**, *39*, 221.
(50) Nogales, A.; Sauer, B. B. *J. Polym. Sci., Part B: Polym. Phys.* **1998**, *36*, 913.
(51) Jiang, Z.; Hutchinson, J. M.; Imrie, C. T. *Polym. Int.* **1998**, *47*, 72.
(52) Endo, R.; Takeda, M. *J. Polym. Sci.* **1962**, *56*, S28.
(53) Schindler, A.; Harper, D. *J. Polym. Sci., Polym. Chem. Ed.* **1979**, *17*, 2593.
(54) Dorgan, J. R.; Williams, J. S.; Lewis, D. N. *J. Rheol.* **1999**, *43*, 1141.
(55) Grijpma, D. W.; Penning, J. P.; Pennings, A. J. *Colloid Polym. Sci.* **1994**, *272*, 1068.
(56) Yang, X.; Kang, S.; Hsu, S. L.; Stidham, H. D.; Smith, P. B.; Leugers, A. *Macromolecules* **2001**, *34*, 5037.
(57) McKenna, G. B.; Simon, S. L. The Glass Transition: Its Measurement and Underlying Physics. In *Handbook of Thermal Analysis and Calorimetry*; Cheng, S. Z. D., Ed.; Elsevier: Amsterdam, 2002; Vol. 3.
(58) Urayama, H.; Kanamori, T.; Kimura, Y. *Macromol. Mater. Eng.* **2001**, *286*, 705.
(59) Fischer, E. W.; Sterzel, H. J.; Wegner, G. *Kolloid Z. Z. Polym.* **1973**, *251*, 980.
(60) Arbe, A.; Colmenero, J.; Monkenbusch, M.; Richter, D. *Phys. Rev. Lett.* **1998**, *81*, 590.
(61) Richter, D.; Monkenbusch, M.; Allgeier, J.; Arbe, A.; Colmenero, J.; Farago, B.; Bae, Y. C.; Faust, R. *J. Chem. Phys.* **1999**, *111*, 6107.
(62) Hoffmann, S.; Willner, L.; Richter, D.; Arbe, A.; Colmenero, J.; Farago, B. *Phys. Rev. Lett.* **2000**, *85*, 772.
(63) Farago, B.; Arbe, A.; Colmenero, J.; Faust, R.; Buchenau, U.; Richter, D. *Phys. Rev. E* **2002**, *65*, 051803.
(64) Arbe, A.; Colmenero, J.; Richter, D.; Monkenbusch, M.; Willner, L.; Farago, B. *Pramana* **2004**, *63*, 33.
(65) Richter, D.; Monkenbusch, M.; Willner, L.; Arbe, A.; Colmenero, J.; Farago, B. *Europhys. Lett.* **2004**, *66*, 239.